

We are IntechOpen, the world's leading publisher of Open Access books Built by scientists, for scientists

4,800

Open access books available

122,000

International authors and editors

135M

Downloads

Our authors are among the

154

Countries delivered to

TOP 1%

most cited scientists

12.2%

Contributors from top 500 universities



WEB OF SCIENCE™

Selection of our books indexed in the Book Citation Index
in Web of Science™ Core Collection (BKCI)

Interested in publishing with us?
Contact book.department@intechopen.com

Numbers displayed above are based on latest data collected.

For more information visit www.intechopen.com



Microwave Filters

Jiafeng Zhou
University of Bristol
UK

1. Introduction

Filters are two-port networks used to control the frequency response in a system by permitting good transmission of wanted signal frequencies while rejecting unwanted frequencies. Generally there are four types of filters: low-pass, high-pass, band-pass, and band-stop.

Microwave filter design has been a persistent and productive field for investigation from the very beginning of microwave engineering. Nowadays, high performance filters are needed in many microwave systems. Because of the importance of microwave filters, a great deal of material on the theory and design of filters is widely available in the literature. The purpose of this chapter is to introduce the basic theory of microwave filters, to describe how to design practical microwave filters, and to investigate ways of implementing high performance filters for modern communication systems.

2. The lowpass prototype

2.1 The lowpass prototype filters

The lumped-element circuit of an n -order lowpass prototype filter is shown in Fig. 1. The circuit shown in Fig. 1(b) is the dual form of that shown in Fig. 1(a). Both forms give identical responses. In Fig. 1, g_1 to g_n are the values of the inductances or capacitances of the reactive elements. g_0 and g_{n+1} are the values of terminal immittances (usually pure resistances or conductances) of the source and load respectively. The g -values for different types of lowpass filters are given in the following sections.

2.2 Butterworth lowpass prototype filter

A typical Butterworth, or “maximally flat”, lowpass response is shown in Fig. 2. The attenuation characteristic can be expressed by (Matthaei et al. 1980)

$$L_A(\omega') = 10 \log_{10} [1 + \varepsilon^2 \left(\frac{\omega'}{\omega'_c}\right)^{2n}] \quad (1)$$

where ω' is the radian frequency variable, and ω'_c is the frequency of the passband edge, or cut-off frequency, as defined in Fig. 2. The value of ε is given by

$$\varepsilon = \sqrt{10^{\frac{L_{Ar}}{10}} - 1} \tag{2}$$

where L_{Ar} is the attenuation at the cut-off frequency ω'_c , In most cases for Butterworth filters, ω'_c is defined as the frequency of the 3-dB passband edge point. That is, $L_{Ar} = 3$ dB, and $\varepsilon = 1$. The parameter n in equation (1) is the order of the filter, or the number of reactive elements in the circuit.

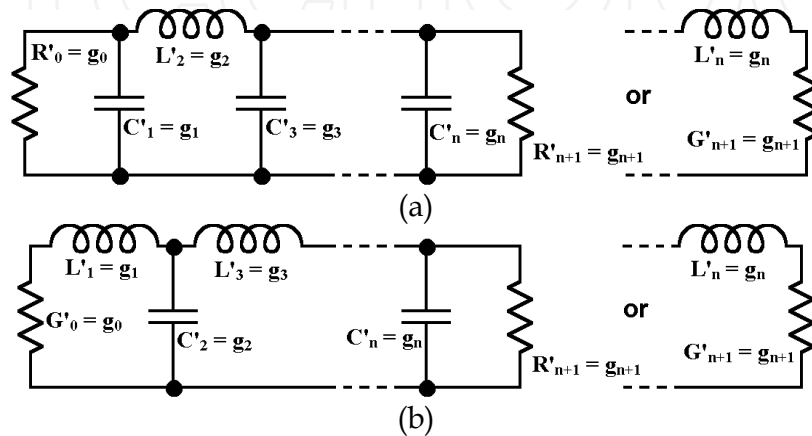


Fig. 1. (a) The prototype of lowpass filters and (b) its dual.

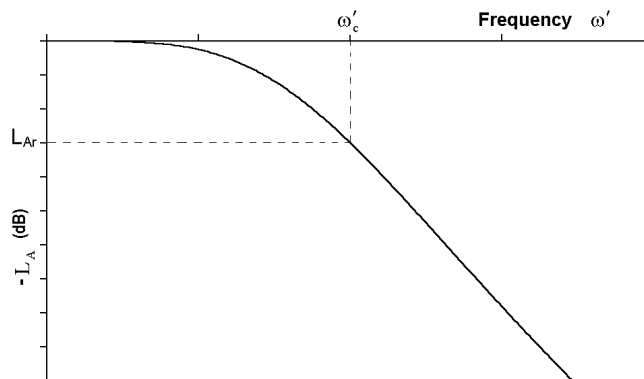


Fig. 2. A typical Butterworth lowpass filter response.

For the Butterworth filters with response of the form shown in Fig. 2, the element values, normalized to make $g_0 = 1$ and $\omega'_c = 1$, can be calculated by

$$g_0 = g_{n+1} = 1$$

$$g_k = 2 \sin\left[\frac{(2k-1)\pi}{2n}\right] \quad (k = 1, 2, \dots, n) \tag{3}$$

The above values can be used to find out the required inductances and capacitances in a real filter having a different cut-off frequency and different terminal impedances (or admittance $Y_0 = 1/Z_0$) by (Matthaei et al. 1980)

$$C_k = \frac{1}{Z_0} \frac{g_k}{\omega'_c} \quad (k \text{ even or odd}) \tag{4}$$

$$L_k = Z_0 \frac{g_k}{\omega'_c} \quad (k \text{ odd or even})$$

where ω'_c is the new cut-off frequency and Z_0 is the new source and load impedance.

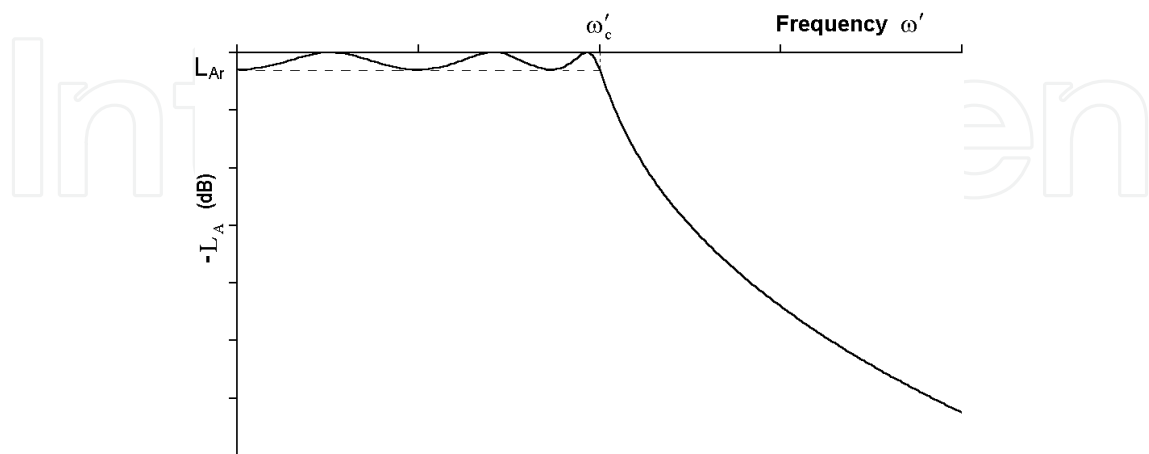


Fig. 3. A typical Chebyshev lowpass filter response (Matthaei et al. 1980) .

2.3 Chebyshev lowpass prototype filter

A typical Chebyshev, or “equal-ripple”, lowpass response is shown in Fig. 3. The attenuation characteristic can be expressed by (Matthaei et al. 1980)

$$L_A(\omega') = 10 \log_{10} \left\{ 1 + \varepsilon^2 \cos^2 \left[n \cos^{-1} \left(\frac{\omega'}{\omega'_c} \right) \right] \right\}, \quad (\text{for } \omega' \leq \omega'_c) \quad (5)$$

$$L_A(\omega') = 10 \log_{10} \left\{ 1 + \varepsilon^2 \cosh^2 \left[n \cosh^{-1} \left(\frac{\omega'}{\omega'_c} \right) \right] \right\}, \quad (\text{for } \omega' \geq \omega'_c)$$

where

$$\varepsilon = \sqrt{10^{\frac{L_{Ar}}{10}} - 1} \quad (6)$$

In this case, L_{Ar} is the maximum attenuation in the pass band, while ω'_c is the equal-ripple band edge. The parameter n is the order of the filter.

The normalized g -values for an n -order Chebyshev low-pass prototype filter can be calculated as follows:

$$\begin{aligned} g_0 &= 1 \\ g_1 &= \frac{2a_1}{\gamma} \\ g_k &= \frac{4a_{k-1}a_k}{b_{k-1}g_{k-1}} \quad (k = 2, 3, 4, \dots, n) \end{aligned} \quad (7)$$

$$g_{n+1} = \coth\left(\frac{\beta}{4}\right)^2 \quad (n \text{ even})$$

$$= 1 \quad (n \text{ odd})$$

where

$$\beta = \ln\left(\frac{\sqrt{1+\varepsilon}+1}{\sqrt{1+\varepsilon}-1}\right) \quad (8)$$

$$\gamma = \sinh\left(\frac{\beta}{2n}\right)$$

and

$$a_k = \sin\left[\frac{(2k-1)\pi}{2n}\right], \quad (k=1,2,\dots,n) \quad (9)$$

$$b_k = \gamma^2 + \sin^2\left(\frac{k\pi}{n}\right), \quad (k=1,2,\dots,n)$$

The above values can be used to find the required inductances and capacitances in a real filter to realize different cut-off frequency and source impedance by

$$C_k = \frac{1}{Z_s} \frac{g_k}{\omega'_c} \quad (k \text{ even or odd})$$

$$L_k = Z_s \frac{g_k}{\omega'_c} \quad (k \text{ odd or even}) \quad (10)$$

$$Z_L = \frac{g_{n+1}}{Z_s} \quad (n \text{ even})$$

$$= g_{n+1} Z_s \quad (n \text{ odd})$$

where ω'_c is the new cut-off frequency, Z_s is the new source impedance and Z_L is the load impedance. It should be noticed that, in the prototype filter, the impedances of the source and load could be different for a Chebyshev filter, while they are the same for the Butterworth case.

Compared with a Butterworth filter of the same order, a Chebyshev response has a much sharper cut-off rate at the transition region, and usually a worse group delay distortion.

2.4 Quasi-elliptic lowpass prototype filters

The synthesis procedures of lowpass prototype filters with Butterworth and Chebyshev characteristics are given above. For these two types of responses, all of transmission zeros (attenuation poles) are at infinite frequencies. The inverse Chebyshev filters and elliptic filters have all of the transmission zeros at finite frequencies. They have a much better cut-off rate in the transition region than Butterworth and Chebyshev filters (Rhodes, 1976). However, due to the difficulties in synthesis and realization of the inverse Chebyshev and elliptic filters, it is usually of more interest to develop alternative quasi-elliptic filters, which have transmission zeros at both finite and infinite frequencies (Rhodes & Alseyab, 1980). Especially quasi-elliptic filters with a single transmission zero (or a pair of transmission

zeros for the transformed bandpass filters) at finite frequency are very attractive. This is not only because these filters can be exactly synthesized and physically realized with little practical difficulty, but also because they give important improvements compared with conventional Butterworth and Chebyshev filters (Levy, 1976). The typical response of quasi-elliptic filters is shown in Fig. 4. The response of such filters has a generalized Chebyshev equal-ripple passband, and a different stopband with transmission zero(s). In filter realization, the transmission zero(s) are usually implemented by cross coupling a pair of nonadjacent elements of the filters.

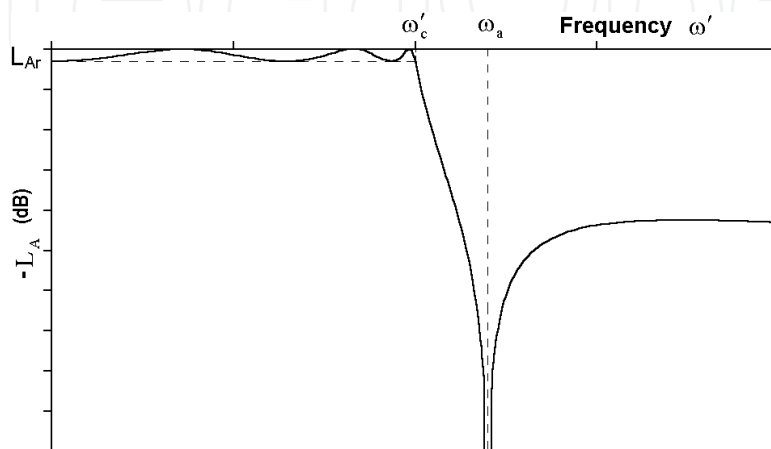


Fig. 4. A typical quasi-elliptic lowpass filter response (Rhodes & Aloseyab, 1980).

The attenuation characteristic of an n -order lowpass prototype filter with a single transmission zero at finite can be expressed by (Rhodes & Aloseyab, 1980)

$$L_A = 1 + \varepsilon^2 F_n^2(\omega') \tag{11}$$

where ε is given by equation (6) and the transfer function is given by

$$F_n(\omega') = \cosh\left[\cosh^{-1} \omega' + (n-1)\cosh^{-1}\left(\omega' \sqrt{\frac{\omega_a^2 - 1}{\omega_a^2 - \omega'^2}}\right)\right] \tag{12}$$

where n is an odd number, and the transmission zeros are at $\omega' = \pm\omega_a$ and infinity. The transmission zero at $\omega' = \omega_a$ is shown in Fig. 4, while the other one $\omega' = -\omega_a$ is the mirror image of the positive one.

Another similar form of the transfer function is given by (Hong & Lancaster, 2000),

$$F_n(\omega') = \cosh\left[(n-2)\cosh^{-1} \omega' + \cosh^{-1}\left(\frac{\omega'\omega_a - 1}{\omega_a - \omega'}\right) + \cosh^{-1}\left(\frac{\omega'\omega_a + 1}{\omega_a + \omega'}\right)\right] \tag{13}$$

where the transmission zeros are at $\omega' = \pm\omega_a$ and infinity. Some useful quasi-elliptic filters have been synthesized in the reference (Hong & Lancaster, 2000).

The general synthesis process to find the values of elements in the prototype quasi-elliptic lowpass filter has been given in the references (Rhodes & Aloseyab, 1980; Levy, 1976).

However, the exact synthesis procedure is quite complicated, and there does not exist closed-form formulas for the element values of quasi-elliptic filters as those for Butterworth and Chebyshev filters. Instead, a set of data is tabulated in the reference (Hong & Lancaster, 2000) for practical design of quasi-elliptic filters up to eighth-order.

3. The lowpass to bandpass transformation

In this section, only Chebyshev lowpass and bandpass filters are discussed. Butterworth and quasi-elliptic filters can be studied in a similar manner. The lowpass prototype shown in Fig. 1(a) is used for the discussion, while the result will be the same if Fig. 1(b) were used instead. The transformation from lowpass to highpass and bandstop filters can be accomplished similarly.

A typical Chebyshev bandpass filter response is shown in Fig. 5. The response can be related exactly to a corresponding lowpass prototype filter by the lowpass to bandpass mapping (Matthaei et al. 1980; Hong & Lancaster, 2001; Collin, 2001)

$$\frac{\omega'}{\omega'_c} = \frac{\omega_0}{\omega_2 - \omega_1} \left(\frac{\omega}{\omega_0} - \frac{\omega_0}{\omega} \right) \quad (14)$$

where ω', ω'_c are the frequency variable and the cut-off frequency of the lowpass prototype filter defined in the above sections respectively. ω_1 and ω_2 are the cut-off frequencies of the passband, and the centre frequency ω_0 is given by

$$\omega_0 = \sqrt{\omega_1 \omega_2} \quad (15)$$

Equation (14) may be solved for ω , giving

$$\omega = \frac{\omega'}{\omega'_c} \frac{\omega_2 - \omega_1}{2} \pm \frac{1}{2} \sqrt{\left(\frac{\omega'}{\omega'_c} \right)^2 (\omega_2 - \omega_1)^2 + 4\omega_1 \omega_2} \quad (16)$$

The point $\omega' = 0$ of the lowpass filter is seen to map into the points $\omega = \pm\omega_0$ of the transformed filter, and $\omega' = \pm\omega'_c$ map into four points $\omega = \pm\omega_1$ and $\omega = \pm\omega_2$. Thus the lowpass band of the prototype filter maps into the passband extending from ω_1 to ω_2 and $-\omega_1$ to $-\omega_2$, which represents bandpass filters with cut-off frequencies at $\pm\omega_1$ and $\pm\omega_2$. The centre frequency $\omega = \pm\omega_0$ is the geometric mean of the cut-off frequencies. The transformed response for $\omega > 0$ is shown in Fig. 5, and the response for $\omega < 0$ is the mirror image of the positive one.

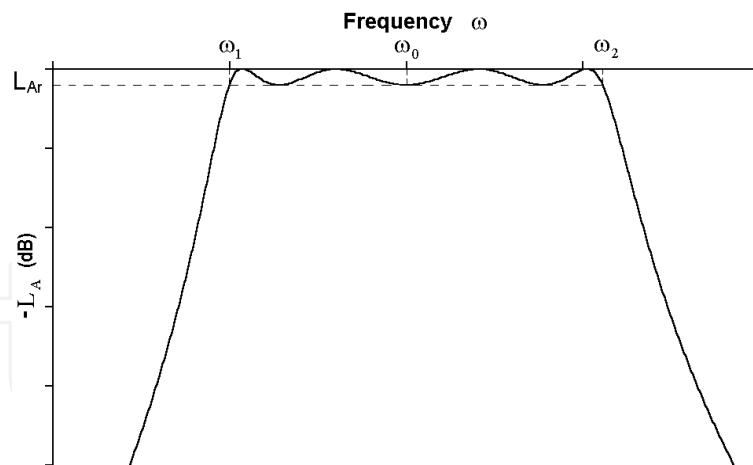


Fig. 5. A typical Chebyshev bandpass filter response.

According to equation (14), to obtain the transformed bandpass response, the shunt capacitance in the prototype lowpass filter needs to be changed to a new susceptance

$$\begin{aligned}
 jB_k &= j\left[\frac{\omega'_c \omega_0}{\omega_2 - \omega_1} \left(\frac{\omega}{\omega_0} - \frac{\omega_0}{\omega}\right)\right] g_k \\
 &= j\omega \left(\frac{\omega'_c g_k}{\omega_2 - \omega_1}\right) + \frac{1}{j\omega \left(\frac{\omega_2 - \omega_1}{\omega'_c \omega_1 \omega_2 g_k}\right)} \quad (k \text{ odd})
 \end{aligned} \quad (17)$$

which is equivalent to a shunt tuned resonator with a shunt capacitance C_k and a shunt inductance L_k given by

$$\begin{aligned}
 C_k &= \frac{\omega'_c g_k}{\omega_2 - \omega_1} \\
 L_k &= \frac{\omega_2 - \omega_1}{\omega'_c \omega_1 \omega_2 g_k} \quad (k \text{ odd})
 \end{aligned} \quad (18)$$

Similarly, the series inductance in the prototype filter should to be changed to a new reactance

$$\begin{aligned}
 jX_k &= j\left[\frac{\omega'_c \omega_0}{\omega_2 - \omega_1} \left(\frac{\omega}{\omega_0} - \frac{\omega_0}{\omega}\right)\right] g_k \\
 &= j\omega \left(\frac{\omega'_c g_k}{\omega_2 - \omega_1}\right) + \frac{1}{j\omega \left(\frac{\omega_2 - \omega_1}{\omega'_c \omega_1 \omega_2 g_k}\right)} \quad (k \text{ odd})
 \end{aligned} \quad (19)$$

which is equivalent to a series tuned resonator with a series capacitance C_k and a series inductance L_k given by

$$C_k = \frac{\omega_2 - \omega_1}{\omega'_c \omega_1 \omega_2 g_k} \quad (20)$$

$$L_k = \frac{\omega'_c g_k}{\omega_2 - \omega_1} \quad (\text{k even})$$

The equivalent circuit of the transformed bandpass filter is shown in Fig. 6.

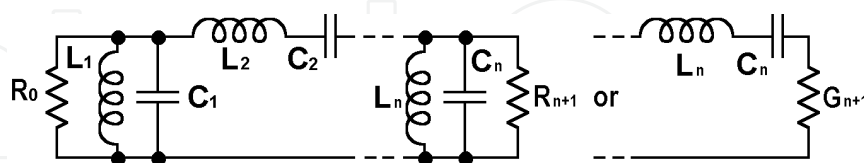


Fig. 6. The equivalent circuit of a bandpass filter transformed from a lowpass filter.

4. Transformation of bandpass filter using K- or J-inverters

The filter shown in Fig. 6 consists of series tuned resonators alternating with shunt-tuned resonators. According to equation (18) and equation (20), such a filter is difficult to implement, because the values of the components are very different in the shunt and series tuned resonators. A way to modify the circuit is to use J - (admittance) or K - (impedance) inverters, so that all resonators can be of the same type.

4.1 Impedance and admittance inverters

An idealized *impedance inverter* operates like a quarter-wavelength line of characteristic impedance K at all frequencies. As shown in Fig. 7(a), if an impedance inverter is loaded with an impedance of Z at one end, the impedance Z_K seen from the other end is (Matthaei et al. 1980)

$$Z_K = \frac{K^2}{Z} \quad (21)$$

An idealized *admittance inverter*, which operates like a quarter-wavelength line with a characteristic admittance Y at all frequencies, is the admittance representation of the same thing. As shown in Fig. 7(b), if the admittance inverter is loaded with an admittance of Y at one end, the admittance Y_J seen from the other end is (Matthaei et al. 1980)

$$Y_J = \frac{J^2}{Y} \quad (22)$$

It is obvious that the loaded admittance Y can be converted to an arbitrary admittance by choosing an appropriate J value. Similarly, the loaded impedance Z can be converted to an arbitrary impedance by choosing an appropriate K value.

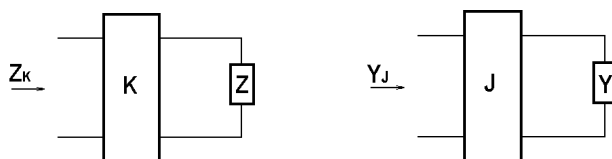


Fig. 7. Definition of K- (impedance) and J- (admittance) inverters.

As indicated above, both the impedance and admittance inverters are like ideal quarter-wave transformers. While K denotes the characteristic impedance of an inverter and J denotes the characteristic admittance of an inverter, there are no conceptual differences in their inverting properties. An impedance inverter with characteristic impedance K is identical to an admittance inverter with characteristic admittance $J = 1/K$. Especially for a unity inverter, with a characteristic impedance of $K = 1$ and a characteristic admittance of $J = 1$.

Besides a quarter-wavelength line, there are some other circuits that operate as inverters. Some useful J - and K -inverters are shown in Fig. 8 and Fig. 9. It should be noticed that some of the inductors and capacitors have negative values. Although it is not practical to realize such components, they will be absorbed by adjacent resonant elements in the filter, as discussed in the following sections. It should also be noted that, since the inverters shown here are frequency sensitive, these inverters are best suitable for narrowband filters. It is shown in the reference (Matthaei et al. 1980) that, using such inverters, filters with bandwidths as great as 20 percent are achievable using half-wavelength resonators, or up to 40 percent by using quarter-wavelength resonators.



Fig. 8. Some circuits useful as J-Inverters.



Fig. 9. Some circuits useful as K-Inverters.

4.2 Conversion of shunt tuned resonators to series tuned resonators

Because of the inverting characteristic indicated by equation (22), a shunt capacitance with a J -inverter on each side acts like a series inductance (Matthaei et al. 1980). Likewise, a shunt tuned resonator with a J -inverter on each side acts like a series tuned resonator. To verify this, a shunt tuned resonator, consisting of a capacitor C and an inductor L , with a J -inverter on each side is shown in Fig. 10(a). Both J -inverters have a value of J . If the circuit is loaded with admittance Y_0 of an arbitrary value at one end, from equation (22), the admittance Y looking in at the other end is given by

$$Y = \frac{J^2}{j\omega C + \frac{1}{j\omega L} + \frac{J^2}{Y_0}} \tag{23}$$

The impedance is, therefore,

$$Z = \frac{1}{Y} = \frac{j\omega C}{J^2} + \frac{1}{j\omega L J^2} + \frac{1}{Y_0} \quad (24)$$

This impedance is equivalent to a series tuned resonator loaded with an impedance of $Z_0 = 1/Y_0$, as shown in Fig. 10(b). The capacitor of C_1 and inductor L_1 of the equivalent circuit are given by

$$\begin{aligned} L_1 &= \frac{C}{J^2} \\ C_1 &= L J^2 \end{aligned} \quad (25)$$

Because the above equations are correct regardless the value of the load Y_0 , the two circuits shown in Fig. 10 are equivalent to each other.

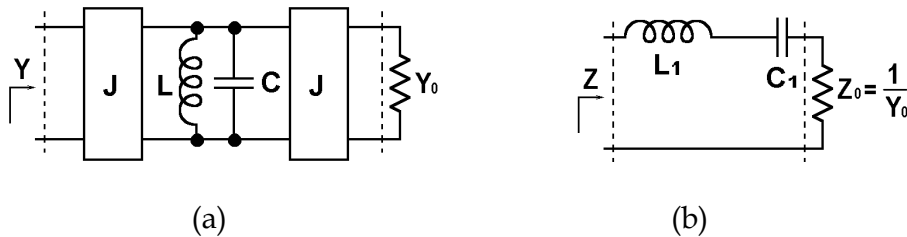


Fig. 10. A shunt tuned resonator with J-inverters on both sides and its equivalent circuit.

It is very useful for the discussion in the following sections to point out that, from equation (25), the transformed resonator can have an arbitrary impedance level $\sqrt{L_1/C_1}$ tuned at the same frequency. That is, the shunt tuned circuit with J-inverters shown in Fig. 10(a) can be converted to a series tuned resonator with an arbitrary L_1 or C_1 , as long as $L_1 C_1 = LC$, by choosing the inverter

$$J = \sqrt{\frac{C}{L_1}} \quad (26)$$

Thus, the bandpass filter shown in Fig. 6 can be converted to a circuit with only shunt resonators by using J-inverters, as shown in Fig. 11.

The dual case of a series tuned resonator with a K-inverter on each side can be derived in a similar manner.

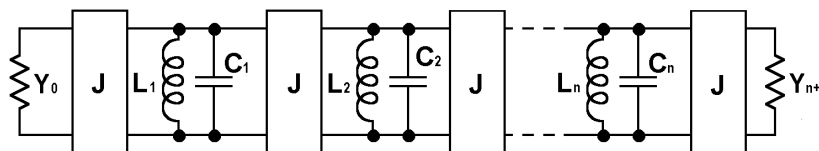


Fig. 11. The bandpass filter using only shunt resonators and J-inverters.

4.3 Conversion of shunt resonators with different J-inverters

In the above section, the shunt-tuned resonator is converted into a series tuned resonator by J-inverters of the same value at both ends. More generally, the inverters may have different values. Fig. 12(a) shows a shunt-tuned circuit with J-inverters at both ends. The resonator consists of a capacitor C and an inductor L. The J-inverters have a value of J_1 on one end and J_2 on the other. This circuit can be transformed to an equivalent circuit shown in Fig. 12(b), where the shunt tuned resonator has a capacitor C' and an inductor L' , whereas $LC=L'C'$, and the J-inverters have values of J'_1 and J'_2 respectively.

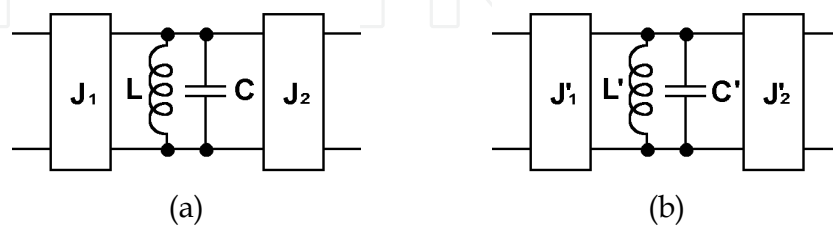


Fig. 12. (a) A shunt tuned resonator with J-inverters of different values, and (b) its equivalent circuit.

The circuit shown in Fig. 12(a) is not symmetrical. If the circuit is loaded with an admittance of Y_{0R} at the right-hand-side end, the admittance Y_L and impedance Z_L looking in at the left-hand-side end are given by

$$Y_L = \frac{J_1^2}{j\omega C + \frac{1}{j\omega L} + \frac{J_2^2}{Y_{0R}}} \quad (27)$$

$$Z_L = \frac{1}{Y_L} = \frac{j\omega C}{J_1^2} + \frac{1}{j\omega L J_1^2} + \frac{J_2^2}{J_1^2 Y_{0R}}$$

Similarly, if the circuit is loaded with an admittance of Y_{0L} at the left-hand-side end, the impedance Z_R looking in at the other end are given by

$$Z_R = \frac{1}{Y_R} = \frac{j\omega C}{J_2^2} + \frac{1}{j\omega L J_2^2} + \frac{J_1^2}{J_2^2 Y_{0L}} \quad (28)$$

In a similar manner, with a load at the one end, the impedance from the other end of the circuit shown in Fig. 12(b) can be given by

$$Z'_L = \frac{1}{Y'_L} = \frac{j\omega C'}{J_1'^2} + \frac{1}{j\omega L' J_1'^2} + \frac{J_2'^2}{J_1'^2 Y_{0R}} \quad (29)$$

And

$$Z'_R = \frac{1}{Y'_R} = \frac{j\omega C'}{J_2'^2} + \frac{1}{j\omega L' J_2'^2} + \frac{J_1'^2}{J_2'^2 Y_{0L}} \quad (30)$$

If the two circuits shown in Fig. 12 are equivalent, $ZL \equiv ZL'$ and $ZR \equiv ZR'$, from equation (27) to equation (30), it can be obtained

$$\begin{aligned} J'_1 &= J_1 \sqrt{\frac{C'}{C}} = J_1 \sqrt{\frac{L}{L'}} \\ J'_2 &= J_2 \sqrt{\frac{C'}{C}} = J_2 \sqrt{\frac{L}{L'}} \end{aligned} \quad (31)$$

This transformation is very useful in a sense that the bandpass the filter shown in Fig. 11 can be further converted to a circuit where all of the resonators have the same inductance and capacitance. Such conversion will be shown in the next section.

4.4 Filter using the same resonators and terminal admittances

In filter design, it is usually desirable to use the same resonators in a filter, and have the same characteristic impedances or admittances at the source and load. In this section, an n -th order bandpass filter will be transformed to use the same shunt resonators tuned at the same frequency, with an inductance of L_0 and a capacitance of C_0 , and the same terminal admittances Y_0 at both ends.

The equivalent circuit of a bandpass filter using only shunt resonators and J-inverters is shown in Fig. 11. As discussed in section 0, the admittance of the source and the load can be converted to the same value Y_0 by adding a J-inverter, or changing the value of the J-inverter if there is a J-inverter directly connected to the source or load. By the transformation discussed in section 0, the circuit shown in Fig. 11 can be transformed to Fig. 13, where all resonators have the same inductances L_0 and capacitance C_0 . The values of the inverters are given by:

$$\begin{aligned} J_{0,1} &= \sqrt{\frac{Y_0 \omega_0 C_0 \Delta}{g_0 g_1 \omega'_c}} \\ J_{n,n+1} &= \sqrt{\frac{Y_0 \omega_0 C_0 \Delta}{g_n g_{n+1} \omega'_c}} \end{aligned} \quad (32)$$

$$J_{k,k+1} = \frac{\omega_0 C_0 \Delta}{\omega'_c} \sqrt{\frac{1}{g_k g_{k+1}}} \quad (k = 1, 2, \dots, n-1)$$

where Δ is the fractional bandwidth of the bandpass filter given by

$$\Delta = \frac{\omega_2 - \omega_1}{\omega_0} \quad (33)$$

where ω_1 , and ω_2 are the cut-off frequencies, and ω_0 is the centre frequency of the filter as defined in equation (15). The values of $g_0, g_1, g_2 \dots g_{n+1}$ and ω'_c are defined in the low-pass prototype filter discussed above.

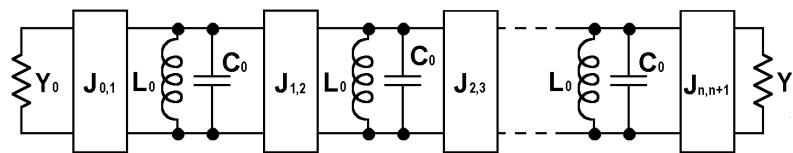


Fig. 13. A transformed bandpass filter using the same resonators.

The above equations are based on the lumped-element equivalent circuit of the filter. More generalized form of these equations will be given in section 0. This transformation is very useful because all the resonators in the filter have the same characteristics, which makes the design and fabrication of the filter much easier. The above transformation can also be implemented by using series tuned resonators and K -inverters in a similar manner.

5. Coupled-resonator filter

The J -inverters in the filter shown in Fig. 13 can be replaced by any of the equivalent circuits shown in Fig. 8 or other equivalent circuits. One form of such filters is shown in Fig. 14, using the equivalent circuit shown in Fig. 8(b) for those J -inverters. The results of this section would still hold if other equivalent circuit were chosen for the inverters.

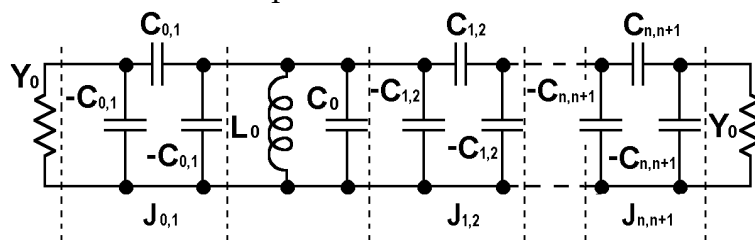


Fig. 14. The transformed filter using the same resonators with capacitive couplings between resonators.

In the filter shown in Fig. 14, the equivalent circuit of each J -inverter consists of one positive series capacitor and two negative shunt ones. In filter design, the positive capacitance represents the mutual capacitances between resonators, while the negative capacitors can be absorbed into the positive shunt capacitors in the resonators. It should be noted that the negative capacitances adjacent to the source and load cannot be absorbed this way. Further discussion about these negative capacitances will be given below in section 0. From equation (32), it is obvious that the knowledge of the equivalent circuit of the resonators will be needed to find out the values of the required J -inverters, whilst the g-values can be obtained from the low-pass prototype filter. Once the values of the J -inverters are determined, the required mutual capacitances between resonators can then be calculated by the equation shown in Fig. 8(b). It should be noted that, as indicated in section 0, the inverters shown in Fig. 8 are actually frequency dependent. However, in the narrow-bandwidth near the centre frequency, the inverters can be regarded as frequency insensitive by approximating

$$J_{k,k+1}(\omega) = \omega C_{k,k+1} \approx \omega_0 C_{k,k+1} \tag{34}$$

where $\omega_0 = 1/\sqrt{L_0 C_0}$, and L_0, C_0 , and $C_{k,k+1}$ are defined in Fig. 14.

5.1 Internal and external coupling coefficients

Due to the distributed-element nature of microwave circuits, it is usually difficult to find out the equivalent circuit of the resonators directly. It is therefore difficult to determine the required values of the J -inverters, or mutual capacitances between resonators. However, from equation (32), it is possible to obtain the required ratio of the mutual capacitance to the shunt capacitance of each resonator without the knowledge of the equivalent circuit. For example, the ratio of the required mutual capacitance between resonators to the capacitance of each resonator is, from equation (32) and equation (34),

$$M_{k,k+1} = \frac{C_{k,k+1}}{C_0} = \frac{\omega_0 C_{k,k+1}}{\omega_0 C_0} \approx \frac{J_{k,k+1}}{\omega_0 C_0} = \frac{\Delta}{\omega'_c} \sqrt{\frac{1}{g_k g_{k+1}}} \quad (k = 1, 2, \dots, n-1) \quad (35)$$

where Δ is the fractional bandwidth of the bandpass filter, and ω'_c, g_k, g_{k+1} are defined in the prototype lowpass filter. $M_{k,k+1}$ is the strength of the internal coupling, or the *coupling coefficient*, between resonators.

The external couplings between the terminal resonators and the source and load are defined in a similar manner by, with the approximation of equation (34),

$$Q_{e0,1} = \frac{Y_0 C_0}{\omega_0 C_{0,1}^2} \approx \frac{\omega_0 C_0 Y_0}{J_{0,1}^2} = \frac{g_0 g_1 \omega'_c}{\Delta} \quad (a) \quad (36a)$$

$$Q_{en,n+1} = \frac{Y_0 C_0}{\omega_0 C_{n,n+1}^2} \approx \frac{\omega_0 C_0 Y_0}{J_{n,n+1}^2} = \frac{g_n g_{n+1} \omega'_c}{\Delta} \quad (b) \quad (36b)$$

The values of $Q_{e0,1}$ and $Q_{en,n+1}$ are the strength of the external couplings, or the *external quality factors*, between the terminal resonators and the source/load.

It can be seen from equation (35) and equation (36) that these required internal and external couplings can be obtained directly from the prototype low-pass filter and the passband details of the transformed bandpass filter, without specific knowledge of the equivalent circuit of the resonators. From equation (32), it can be proved that fixing the internal and external couplings as prescribed by equation (35) and equation (36) is adequate to fix the response of the filter shown in Fig. 14 (Matthaei et al. 1980). The following two sections will concentrate on experimentally determining these couplings.

5.2 Determination of internal couplings by simulation

After finding the required coupling coefficients and external quality factors for the desired filtering characteristics as discussed above, it is essential to experimentally determine these couplings in a practical circuit so as to find the dimensions of the filter for fabrication. This section describes the determination of the coupling coefficients between resonators by the use of full wave simulation. The details about the external couplings between the terminal resonators and the source and load are given in the next section.

As discussed above, the same resonators are usually used in a filter. The equivalent circuit of a pair of coupled identical resonators is shown in Fig. 15, which can be regarded as part

of the filter shown in Fig. 14. As the circuit is symmetrical, the admittance looking in at either side is,

$$Y_{in} = \frac{1}{j\omega L_0} + j\omega(C_0 - C_{k,k+1}) + \frac{1}{\frac{1}{j\omega C_{k,k+1}} + \frac{1}{j\omega(C_0 - C_{k,k+1}) + \frac{1}{j\omega L_0}}} \quad (37)$$

At resonance, $Y_{in}=0$. By equating the right-hand side of equation (37) to zero, four eigenvalues of the frequency ω can be obtained. The two positive frequencies are given by

$$\begin{aligned} \omega_{01} &= \frac{1}{\sqrt{L_0(C_0 + C_{k,k+1})}} \\ \omega_{02} &= \frac{1}{\sqrt{L_0(C_0 - C_{k,k+1})}} \end{aligned} \quad (38)$$

The other two negative frequencies are the mirror image of these positive ones.

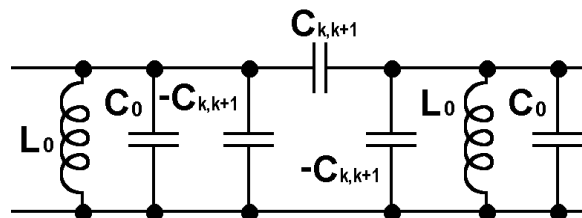


Fig. 15. The equivalent circuit of a pair of coupled identical resonators.

If this circuit is weakly coupled to the exterior ports for measurement or simulation, the typical measured or simulated response for the scattering parameter S_{21} is as shown in Fig. 16. More details of the measurement or simulation will be given in the next section. The two resonant frequencies as expressed in equation (38) are specified in Fig. 16. By inspecting equation (35) and equation (38), the coupling coefficient can be determined by,

$$M_{k,k+1} = \frac{C_{k,k+1}}{C_0} = \frac{\omega_{02}^2 - \omega_{01}^2}{\omega_{02}^2 + \omega_{01}^2} \approx \frac{\omega_{02} - \omega_{01}}{\omega_0} \quad (k = 1, 2, \dots, n-1) \quad (39)$$

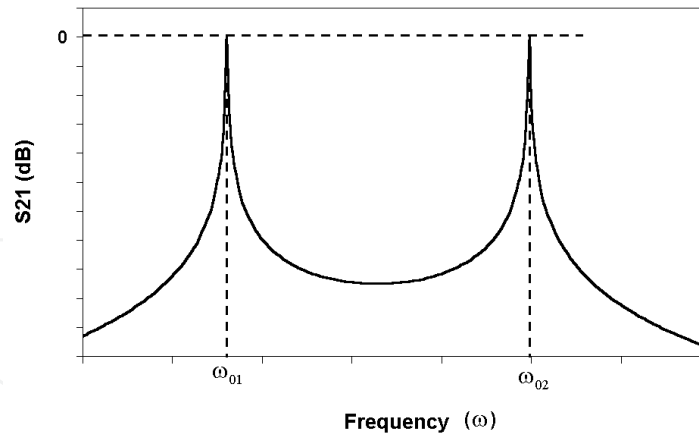


Fig. 16. A typical response of the coupled resonators shown in Fig. 15.

5.3 Determination of external couplings by simulation

The procedure to determine the strength of the external coupling, the external quality factor Q_e , is somewhat different from determining the internal coupling coefficient between resonators. It is possible to take the corresponding part of the circuit, for example, the load, the last resonator and the inverter between them, from Fig. 14, and determine the external quality factor by measuring the phase shift of group delay of the selected circuit (Hong & Lancaster, 2001).

More conveniently, a doubly loaded resonator shown in Fig. 17 is considered. One end of the circuit is the same as in Fig. 14, while another load and inverter of the same values are added symmetrically at the other end. The ABCD matrix of the whole circuit, except the two loads, is given by

$$\begin{pmatrix} A_Q & B_Q \\ C_Q & D_Q \end{pmatrix} = \begin{pmatrix} 0 & \frac{1}{j\omega C_e} \\ -j\omega C_e & 0 \end{pmatrix} \begin{pmatrix} 1 & 0 \\ j\omega C_0 + \frac{1}{j\omega L_0} & 1 \end{pmatrix} \begin{pmatrix} 0 & \frac{1}{j\omega C_e} \\ -j\omega C_e & 0 \end{pmatrix} \quad (40)$$

where $C_e = C_{0,1}$, or $C_{n,n+1}$ as defined in Fig. 14. The scattering parameter S_{21} can be calculated by

$$S_{21} = \frac{2}{A_Q + Y_0 B_Q + \frac{C_Q}{Y_0} + D_Q} = \frac{2}{-2 - \frac{jY_0}{\omega^2 C_e^2} (\omega C_0 - \frac{1}{\omega L_0})} \quad (41)$$

By substituting equation (36) and $\omega_0 = 1/\sqrt{L_0 C_0}$, this equation can be rewritten as

$$S_{21} = \frac{-2}{2 + \frac{jY_0 \omega_0 C_0}{\omega^2 C_e^2} (\frac{\omega}{\omega_0} - \frac{\omega_0}{\omega})} = \frac{-2}{2 + jQ_e (\frac{\omega}{\omega_0} - \frac{\omega_0}{\omega})} \quad (42)$$

where $Q_e = Q_{0,1}$ or $Q_{n,n+1}$ is the external quality factor for the source or load as defined in equation (36). At a narrow bandwidth around the resonant frequency, $\omega/\omega_0 - \omega_0/\omega \approx 2\Delta\omega/\omega_0$ with $\omega = \omega_0 + \Delta\omega$. The magnitude of S_{21} is given by

$$|S_{21}| = \frac{1}{\sqrt{1 + (Q_e \Delta\omega / \omega_0)^2}} \tag{43}$$

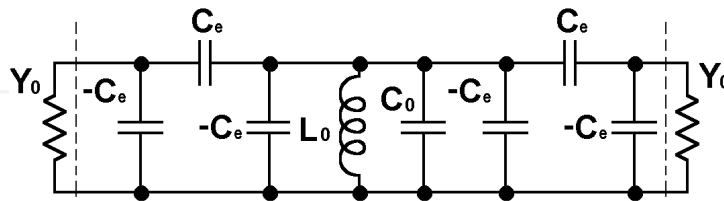


Fig. 17. The equivalent circuit of a doubly loaded resonator.

If this circuit is connected to the exterior ports for measurement or simulation, the typical measured or simulated response of the doubly coupled resonator is shown in Fig. 18. It can be found from equation (43) that $|S_{21}|$ has a maximum value $|S_{21}| = 1$ (or 0 dB) at $\Delta\omega = 0$, and the value falls to 0.707 (or -3 dB) at

$$\frac{Q_e \Delta\omega}{\omega_0} = \pm 1 \tag{44}$$

The two solutions of equation (44) are given by

$$\Delta\omega = \pm \frac{\omega_0}{Q_e} \tag{45}$$

The two corresponding frequencies $\omega_1 = \omega_0 - \omega_0 / Q_e$ and $\omega_2 = \omega_0 + \omega_0 / Q_e$ can be easily found by simulation or measurement as shown in Fig. 18. The external quality factor therefore can be given by

$$Q_e = \frac{\omega_0}{2(\omega_2 - \omega_1)} \tag{46}$$

As indicated above, the external quality factor Q_e is actually defined for a singly loaded resonator. One possible way to determine Q_e of a singly coupled resonator is to measure the phase shift of group delay of the reflection coefficient (S_{11}) of a singly loaded resonator, and the external quality factor is given by (Hong & Lancaster, 2001)

$$Q_e = \left| \frac{\omega_0}{\omega_{+90^\circ} - \omega_{-90^\circ}} \right| \tag{47}$$

where ω_{+90° and ω_{-90° are the frequencies at which the phase shifts are $\pm 90^\circ$ respectively. The external quality factor can also be given by (Hong & Lancaster, 2001)

$$Q_e = \frac{\omega_0 \tau(\omega_0)}{4} \tag{48}$$

where $\tau(\omega_0)$ is the group delay of S_{11} at the centre frequency ω_0 .

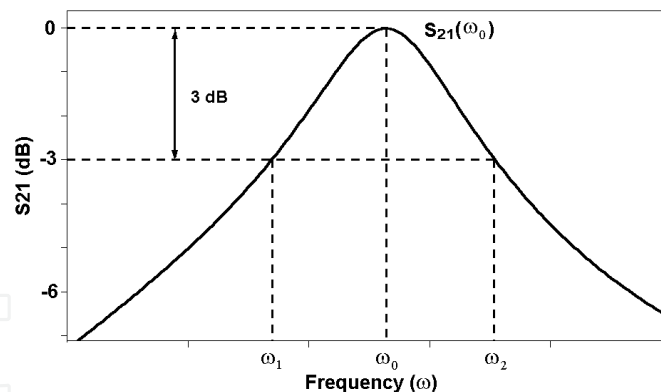


Fig. 18. The typical response of a doubly coupled resonator.

Another more practical way to determine the external quality factor of a singly loaded resonator is to use an equivalent circuit shown in Fig. 19. The circuit is similar to Fig. 14, except that one end of the circuit has the external coupling to be measured, while the other end has a relatively much weaker coupling, namely $C_w \ll C_e$. The ABCD matrix of the circuit can be expressed as, similar to equation (40),

$$\begin{pmatrix} A_{Q1} & B_{Q1} \\ C_{Q1} & D_{Q1} \end{pmatrix} = \begin{pmatrix} 0 & \frac{1}{j\omega C_e} \\ -j\omega C_e & 0 \end{pmatrix} \begin{pmatrix} 1 & 0 \\ j\omega C_0 + \frac{1}{j\omega L_0} & 1 \end{pmatrix} \begin{pmatrix} 0 & \frac{1}{j\omega C_w} \\ -j\omega C_w & 0 \end{pmatrix} \quad (49)$$

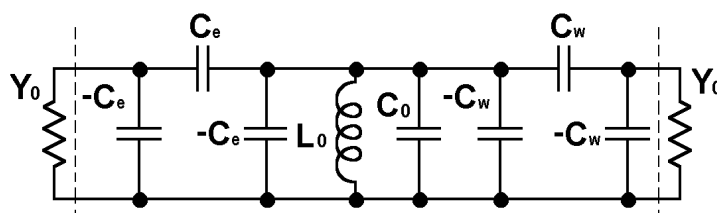


Fig. 19. The equivalent circuit of a singly loaded resonator. It is called “singly” loaded because the coupling at one end, represented by C_e 's, is much stronger than the coupling at the other end, represented by C_w 's.

The scattering parameter S_{21} can be obtained, similarly to equation (42), by

$$S_{21} = \frac{-2}{\left(\frac{C_e}{C_w} + \frac{C_w}{C_e}\right) - j\frac{C_e}{C_w} Q_e \frac{\Delta\omega}{\omega_0}} \quad (50)$$

It is obvious that if $C_w = C_e$, this equation is the same as equation (42). Here as $C_w \ll C_e$, equation (50) can be rewritten as,

$$S_{21} = -\frac{2C_w}{C_e} \frac{1}{\left(1 - j2Q_e \frac{\Delta\omega}{\omega_0}\right)} \quad (51)$$

The typical response of the circuit is very similar to Fig. 18, except that the value of $|S_{21}|$ has a maximum value of $2C_w/C_e$ [or $20\log(2C_w/C_e)$ dB] at $\Delta\omega = 0$. The value is 3 dB lower at frequencies where $\Delta\omega$ is given by,

$$\frac{2Q_e \Delta\omega}{\omega_0} = \pm 1 \quad (52)$$

The two corresponding frequencies are $\omega_1 = \omega_0 - \omega_0/(2Q_e)$ and $\omega_2 = \omega_0 + \omega_0/(2Q_e)$. The external quality factor, therefore, can be determined by

$$Q_e = \frac{\omega_0}{\omega_2 - \omega_1} \quad (53)$$

5.4 Equivalent circuit of the inverters at the source and load

In the above discussion, some negative shunt capacitances are used to realize the inverters. Most of these negative capacitances can be absorbed by the adjacent resonators. However, this absorption procedure does not work for the inverters between the end resonators and the terminations (source and load), as the terminations usually have pure resistances or conductances.

This difficulty can be avoided if another equivalent circuit, shown in Fig. 20, is used for the J -inverter. As indicated above, by using any equivalent circuits to realize the required inverters, the filter response will be the same. All the methods to determine the external quality factor as described by equations (46), (47), (48) and (53) are still valid.

In the circuit shown in Fig. 20, at the resonant frequency, the admittance looking in from the resonator towards the source is given by

$$Y_{in} = j\omega_0 C_a + \frac{1}{\frac{1}{Y_0} + \frac{1}{j\omega_0 C_b}} = \frac{1}{\frac{1}{Y_0} + \frac{Y_0}{\omega_0^2 C_b^2}} + j(\omega_0 C_a + \frac{1}{\frac{Y_0^2}{\omega_0 C_b} + \frac{1}{\omega_0 C_b}}) \quad (54)$$

Because the required value of the J -inverter is $J_e = J_{0,1}$, or $J_{n,n+1}$ as defined in Fig. 13, the required admittance is therefore J_e^2/Y_0 . By equating this value to the real part of Y_{in} , two solutions of C_b can be obtained, and the positive one is given by

$$C_b = \frac{J_e}{\omega_0 \sqrt{1 - \left(\frac{J_e}{Y_0}\right)^2}} \quad (55)$$

By equating the imaginary part of Y_{in} to 0, C_a can be found by

$$C_a = -\frac{C_b}{1 + \left(\frac{\omega_0 C_b}{Y_0}\right)^2} \quad (56)$$

This negative shunt capacitance can be absorbed by the resonator.

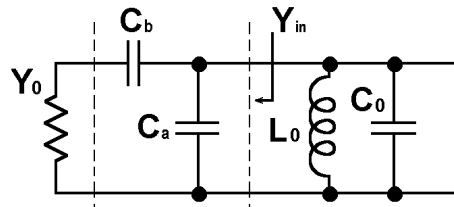


Fig. 20. Another equivalent circuit to realize the inverter between the end resonator and the termination.

5.5 More generalized equations

Since purely lumped elements are difficult to realize at microwave frequencies, it is usually more desirable to construct the resonators in a distributed-element form. Such a resonator can be characterized by its centre frequency ω_0 and its susceptance slope parameter (Matthaei et al. 1980)

$$\ell = \frac{\omega_0}{2} \left. \frac{dB(\omega)}{d\omega} \right|_{\omega_0} \quad (57)$$

where B is the susceptance of the resonator. For a shunt tuned lumped-element resonator, equation (57) can be simplified as $\ell = \omega_0 C = 1/(\omega_0 L)$. The values of J -inverters for filters using distributed-element resonators can be calculated by replacing $\omega_0 C_0$ with ℓ_0 in equation (32), where ℓ_0 is the susceptance slope parameter of the distributed-element resonators. More generally, if the slope parameter of each resonator is different from the others, equation (32) can be rewritten as (Matthaei et al. 1980)

$$J_{0,1} = \sqrt{\frac{Y_0 \ell_1 \Delta}{g_0 g_1 \omega'_c}} \quad (58a)$$

$$J_{n,n+1} = \sqrt{\frac{Y_0 \ell_n \Delta}{g_n g_{n+1} \omega'_c}} \quad (58b)$$

$$J_{k,k+1} = \frac{\Delta}{\omega'_c} \sqrt{\frac{\ell_k \ell_{k+1}}{g_k g_{k+1}}} \quad (k = 1, 2, \dots, n-1) \quad (58c)$$

where ℓ_k is the susceptance slope parameter of k -th resonator, Δ is given in equation (33), and the values of $g_0, g_1, g_2, \dots, g_{n+1}$ and ω'_c are defined in the low-pass prototype filter. The definition of the coupling coefficient equation (35) can be modified to (Matthaei et al. 1980),

$$M_{k,k+1} = \frac{J_{k,k+1}}{\sqrt{\ell_k \ell_{k+1}}} = \frac{\Delta}{\omega'_c} \frac{1}{\sqrt{g_k g_{k+1}}} \quad (k = 1, 2, \dots, n-1) \quad (59)$$

If it is possible to find the equivalent capacitances C_k, C_{k+1} for the k -th and $(k+1)$ -resonators, and the equivalent mutual capacitance $C_{k,k+1}$ in the vicinity of the centre frequency, the coupling coefficient $M_{k,k+1}$ can be expressed by

$$M_{k,k+1} = \frac{J_{k,k+1}}{\sqrt{\ell_k \ell_{k+1}}} \approx \frac{\omega_0 C_{k,k+1}}{\sqrt{\ell_k \ell_{k+1}}} = \frac{C_{k,k+1}}{\sqrt{C_k C_{k+1}}} \quad (k=1,2,\dots,n-1) \quad (60)$$

In a similar manner, equation (36) can be modified to

$$Q_{e0,1} = \frac{\ell_1 Y_0}{J_{0,1}^2} = \frac{g_0 g_1 \omega'_c}{\Delta} \quad (61a)$$

$$Q_{en,n+1} = \frac{\ell_n Y_0}{J_{n,n+1}^2} = \frac{g_n g_{n+1} \omega'_c}{\Delta} \quad (61b)$$

Or, if the equivalent capacitances in the vicinity of the centre frequency of the terminal resonators can be found,

$$Q_{e0,1} = \frac{\ell_1 Y_0}{J_{0,1}^2} \approx \frac{Y_0 C_1}{\omega_0 C_{0,1}^2} \quad (62a)$$

$$Q_{en,n+1} = \frac{\ell_n Y_0}{J_{n,n+1}^2} \approx \frac{Y_0 C_n}{\omega_0 C_{n,n+1}^2} \quad (62b)$$

For the case when a filter uses resonators tuned at different frequencies, the determination of the coupling coefficients are described in Chapter 8 of the reference (Hong & Lancaster, 2001).

6. Design example of a Chebyshev filter

At microwave and millimetre wave frequencies, filters are not usually built by using the lumped-element components as discussed above, but by utilizing transmission lines, usually called distributed-element components. The complex behaviour of the distributed-element components makes it very difficult to develop a complete synthesis procedure for microwave filters. It is, however, possible to approximate the behaviour of ideal capacitors and inductors by using appropriate microwave components in a limited frequency range. Thus the microwave filter is realized by replacing capacitors and inductors in the lumped-element filters by suitable microwave components with similar frequency characteristics in the frequency band of interest. The microwave filter design procedure is further simplified by the aid of CAD program.

6.1 Filter synthesis

In this section, a three-pole Chebyshev bandpass filter with a fractional bandwidth of 0.461% centred at 610 MHz, and a ripple of 0.01dB in the passband, will be designed by simulation (Sonnet Software, 2009) using the above theory.

Firstly, the g -values of the three-pole Chebyshev prototype lowpass filter, with a ripple of 0.01 dB, can be calculated by equation (7): $g_0=1$, $g_1=0.6291$, $g_2=0.9702$, $g_3=0.6291$ and $g_4=1$. Substituting these values with $\omega'_c=1$ and the fractional bandwidth 0.461% into equation (35) and (36) results in,

$$M_{1,2} = M_{2,3} = 0.005901 \quad (63)$$

$$Q_{e0,1} = Q_{e3,4} = 136.5$$

where $M_{1,2}$ and $M_{2,3}$ are the coupling coefficients between resonators, and $Q_{e0,1}$ and $Q_{e3,4}$ are the external factors between the end resonators and the terminations (source and load).

6.2 Determination of the couplings by simulation

The shape and dimensions of a microstrip resonator centred at 610 MHz are shown in Fig. 21. The centre frequency can be tuned in a small range by changing the lengths of the stubs A and B. The resonator is designed on a 0.50 mm thick MgO substrate. More details on the design of this resonator can be found in the reference (Zhou et al., 2005).

To determine the coupling strength between resonators, the structure shown in Fig. 22(a) is used for simulation. The couplings between the resonators and the feed lines are much weaker than that between the two resonators. As discussed in section 0, two resonant frequencies will be obtained from the simulation as shown in Fig. 22(b), similar to Fig. 16. The coupling coefficient can be extracted by using equation (39). The coupling coefficient is a function of the distance d between the resonators, and the relationship between the coupling strength and the distance d is shown in Fig. 23. It can be found in Fig. 23 that two resonators with a distance of 0.60 mm have a coupling coefficient 0.0059, which is very close to the required value of 0.005901.

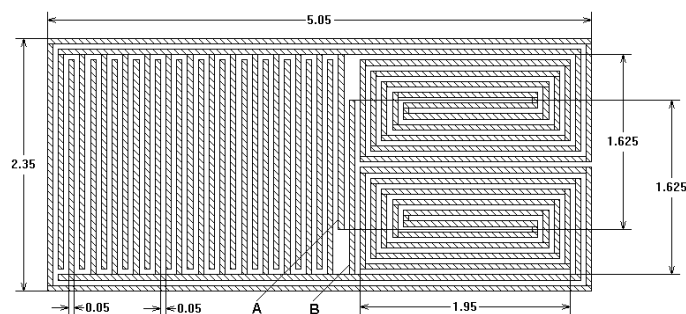


Fig. 21. Layout of the resonator centred at 610 MHz. The minimum line and gap widths are 0.050 mm. Other detailed dimensions are shown in the figure (unit: mm).

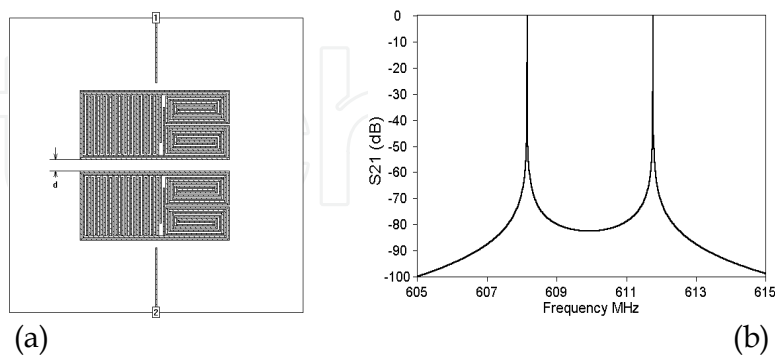


Fig. 22. (a) The structure to determine the coupling strength between resonators in the simulation, and (b) the simulated response for $d = 0.6$ mm.

The external coupling between the end resonator and the termination is realized by a tapped line, as shown in Fig. 24(a). The length t along the signal line of the resonator, from the tapped line to the middle of the resonator, controls the strength of the external coupling. The

resonator is weakly coupled to the other feed line, so that the circuit can be regarded as a singly loaded resonator as discussed in section 0. The wide microstrip line connected to port 1 has a characteristic impedance of 50 ohm, the length of which does not affect the response of the circuit.

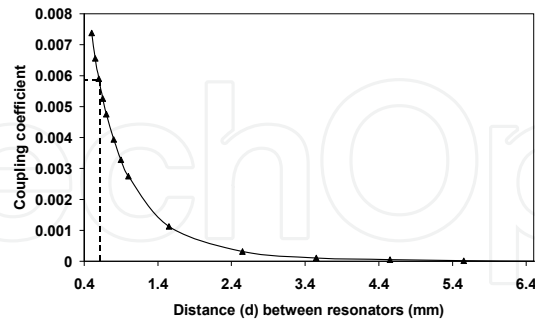


Fig. 23. The coupling coefficient against the distance between the resonators.

The simulated response is shown in Fig. 24(b), similar to Fig. 18, and the external quality factor can be extracted by using equation (53). The relationship between the external quality factor and the length t is shown in Fig. 25. It can be found that $t = 4.2$ mm gives an external Q of 135, which is close to the required value of 136.5.

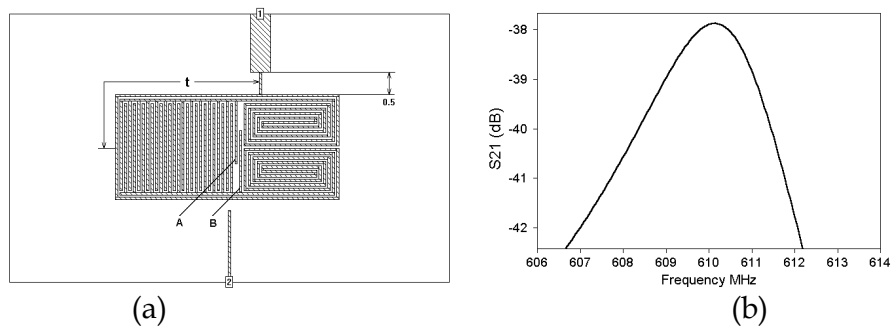


Fig. 24. (a) The structure to determine the external coupling between the end resonator and the termination in the simulation (unit: mm) and (b) the simulated response for $t = 3.9$ mm.

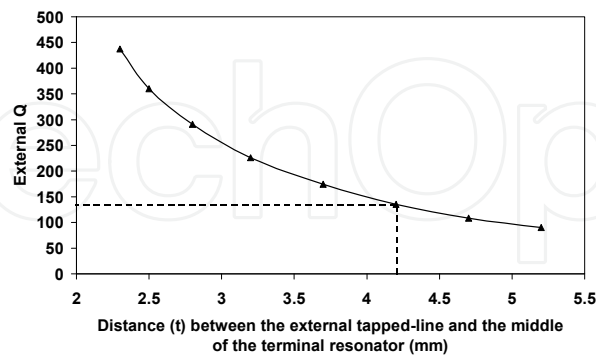


Fig. 25. The external coupling strength against the length from the tapped line to the middle of the resonator.

It should be noted that the position of the tapped line also affects the centre frequency of the end resonator. Therefore the dimensions of the end resonator need to be changed slightly to keep the desired centre frequency. This is done by changing the length of the stubs A and B as shown in Fig. 24.

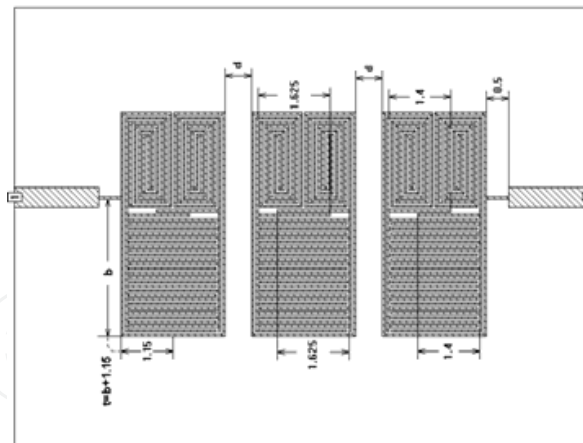


Fig. 26 Layout and dimensions of the three-pole Chebyshev filter (unit: mm), where $t = 4.3$ and $d = 0.60$ after optimisation. More detailed dimensions of the resonators can be found in Fig. 21 and Fig. 24(a).

For the required external Q for this filter, the length of A and B is found to be 1.4 mm, which compares to the length of 1.625 mm in the original resonator shown in Fig. 21.

The filter is formed in a shape as shown in Fig. 26. It will be discussed below that further optimization of the filter is required to achieve optimal performance.

6.3 Circuit optimisation and simulated response

The theoretical response of the three-pole Chebyshev filter designed is shown in Fig. 27. The theoretical response is obtained by calculation using the coupling coefficients given in equation (63). More details on the calculation are given in Chapter 8 of the reference (Hong & Lancaster, 2001).

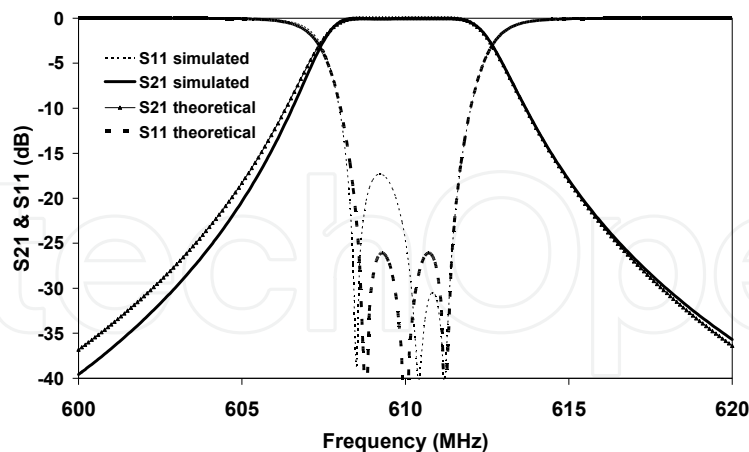


Fig. 27. The theoretical and simulated responses of the three-pole Chebyshev filter.

The dimensions obtained in section 0 are used by the full-wave simulator Sonnet (Sonnet Software, 2009). The simulated response of the filter is shown in Fig. 27. However, the simulated response using these dimensions is close to, but does not meet the theoretical response very well. Generally, there are two major reasons. One reason is that, in the simulator, the dimensions of the circuit are “discrete” rather than “continuous”, so that the

required coupling coefficients can usually be realized proximately, rather than precisely. This is because in the simulator a “cell” is the basic building block of the circuit. Thus any part of the circuit may be as small as one cell or may be multiple cells long or wide. For example, a typical circuit drawn in the simulator is shown in Fig. 28, which has a cell size of $0.05 \text{ mm} \times 0.025 \text{ mm}$. The black dots are the grid points. The dimensions of the circuit in the horizontal direction, such as w and d , can only be the multiple of 0.05 mm ; while the dimensions in the vertical direction, such as h , can only be the multiple of 0.025 mm . If $d = 0.75 \text{ mm}$ would give the required performance, in the simulator, only the proximate value $d = 0.5$ or 1.0 mm could be used. The dimensions can be more precise if the cell size is smaller. But, on the other hand, the simulation time increases exponentially as the cell size decreases.

Another reason is that the unwanted cross couplings, among non-neighbouring resonators and between input and output ports, are not considered in the design. These cross couplings cannot be easily determined before the design as they are not independent to other couplings, and they become much more complicated in a filter having more resonators. Alternatively, the simulator (Sonnet Software, 2009) has an “optimisation function”, which can be used to optimise the dimensions of a circuit to get an optimised performance.

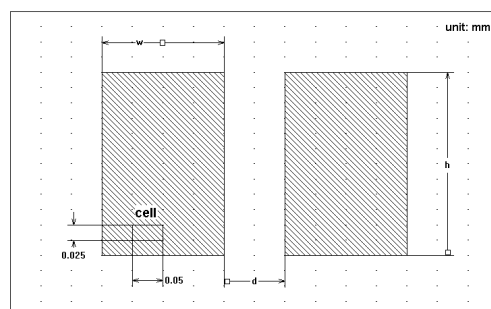
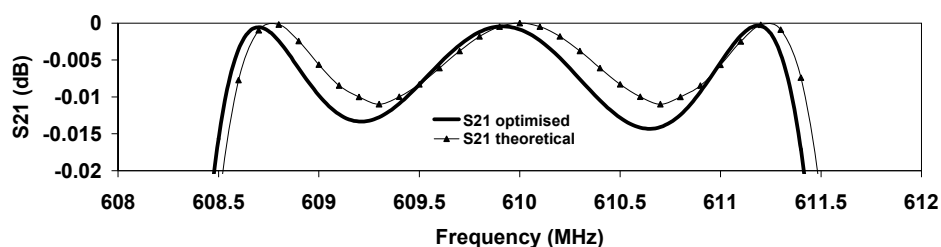


Fig. 28. An example circuit drawn in the EM simulator (Sonnet Software, 2009).

By using this function, the user may select dimensions of the circuit and define them as a parameter. In the analysis, the simulator controls the parameter value, within a user defined range, in an attempt to reach a user defined goal. More than one parameters can be used simultaneously in the simulation if necessary. More detailed information about the optimisation can be found in the reference (Sonnet Software, 2009).

The dimensions of the three-pole filter after optimisation by the simulator are shown in Fig. 26, where $t = 4.3 \text{ mm}$ and $d = 0.60 \text{ mm}$. The optimised response is shown in Fig. 29, which agrees very well with the theoretical result. The optimised passband has a ripple of 0.014 dB , very close to the target of 0.01 dB ; and the minimum return loss is better than 25 dB in the passband, also close to the theoretical value of 26.3 dB .



(a)

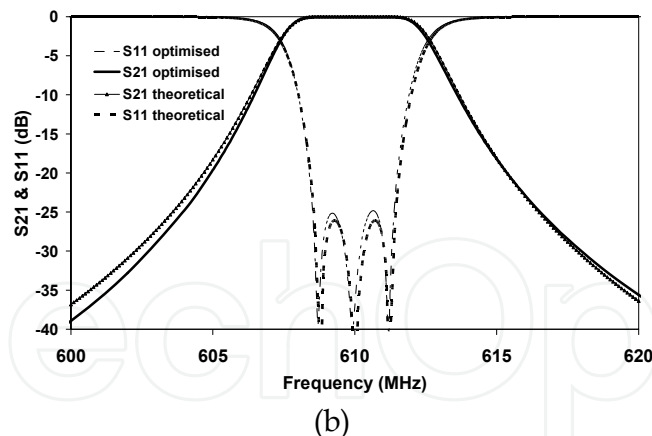


Fig. 29. The theoretical and optimised performances of the 3-pole Chebyshev filter.

7. Summary

The general theory of microwave filter design based on lumped-element circuit is described in this chapter. The lowpass prototype filters with Butterworth, Chebyshev and quasi-elliptic characteristics are synthesized, and the prototype filters are then transformed to bandpass filters by lowpass to bandpass frequency mapping. By using immittance inverters (J - or K -inverters), the bandpass filters can be realized by the same type of resonators. One design example is given to verify the theory on how to design microwave filters.

8. Reference

- Collin R. E. (2001). *Foundation for Microwave Engineering*, John Wiley & Sons, Inc. ISBN: ISBN 0-7803-6031-1. New Jersey.
- Hong, J. S. & Lancaster, M. J. (2000). Design of Highly Selective Microstrip Bandpass Filters with a Single Pair of Attenuation Poles at Finite Frequencies, *IEEE Transactions on Microwave Theory and Technology*, vol. 48, July 2000. pp. 1098-1107.
- Hong, J. S. & Lancaster, M. J. (2001). *Microstrip Filters for RF/Microwave Applications*, John Wiley & Sons, INC. ISBN: 0-471-38877-7, New York.
- Levy, R. (1976). Filters with single transmission zeros at real and imaginary frequencies, *IEEE Transactions on Microwave Theory and Technology*, vol. 24, Apr. 1976. pp. 172-181.
- Matthaei, G.; Young, L. & Jones, E.M.T. (1980). *Microwave Filters, Impedance-matching Networks and Coupling Structure*, Artech House, INC. 685 Canton Street, Norwood, MA 02062.
- Rhodes, J. D. (1976). *Theory of Electrical Filters*, Wiley. ISBN: 0-471-71806-8, New York.
- Rhodes, J. D. & Alesyab, S. A. (1980). The generalized Chebyshev low-pass prototype filter. *Circuit Theory Application*, vol.8, 1980. pp.113-125.
- Sonnet Software (2009), *EM User's Manual*, Sonnet Software, Inc. Elwood Davis Road North Syracuse, NY 13212
- Zhou, J.; Lancaster, M. J.; Huang, F.; Roddis, N. & Glynn, D. (2005) HTS narrow band filters at UHF band for radio astronomy applications, *IEEE Transactions on Applied Superconductivity*, vol.15, June 2005. pp.1004 - 1007.



Microwave and Millimeter Wave Technologies from Photonic Bandgap Devices to Antenna and Applications

Edited by Igor Minin

ISBN 978-953-7619-66-4

Hard cover, 468 pages

Publisher InTech

Published online 01, March, 2010

Published in print edition March, 2010

The book deals with modern developments in microwave and millimeter wave technologies, presenting a wide selection of different topics within this interesting area. From a description of the evolution of technological processes for the design of passive functions in millimetre-wave frequency range, to different applications and different materials evaluation, the book offers an extensive view of the current trends in the field. Hopefully the book will attract more interest in microwave and millimeter wave technologies and simulate new ideas on this fascinating subject.

How to reference

In order to correctly reference this scholarly work, feel free to copy and paste the following:

Jiafeng Zhou (2010). Microwave Filters, Microwave and Millimeter Wave Technologies from Photonic Bandgap Devices to Antenna and Applications, Igor Minin (Ed.), ISBN: 978-953-7619-66-4, InTech, Available from: <http://www.intechopen.com/books/microwave-and-millimeter-wave-technologies-from-photonic-bandgap-devices-to-antenna-and-applications/microwave-filters>

INTECH
open science | open minds

InTech Europe

University Campus STeP Ri
Slavka Krautzeka 83/A
51000 Rijeka, Croatia
Phone: +385 (51) 770 447
Fax: +385 (51) 686 166
www.intechopen.com

InTech China

Unit 405, Office Block, Hotel Equatorial Shanghai
No.65, Yan An Road (West), Shanghai, 200040, China
中国上海市延安西路65号上海国际贵都大饭店办公楼405单元
Phone: +86-21-62489820
Fax: +86-21-62489821

© 2010 The Author(s). Licensee IntechOpen. This chapter is distributed under the terms of the [Creative Commons Attribution-NonCommercial-ShareAlike-3.0 License](#), which permits use, distribution and reproduction for non-commercial purposes, provided the original is properly cited and derivative works building on this content are distributed under the same license.

IntechOpen

IntechOpen